JOURNAL OF GEOPHYSICAL RESEARCH, VOL. 95, NO. A1, PAGES 119–137, JANUARY 1, 1990

Characteristics of Wave-Particle Interactions During Sudden Commencements 1. Ground-Based Observations

W. B. GAIL,[1] U.S. INAN, R. A. HELLIWELL, AND D. L. CARPENTER

Space, Telecommunications, and Radioscience Laboratory, Stanford University, Stanford, California

S. KRISHNASWAMY[2] AND T. J. ROSENBERG

Institute for Physical Science and Technology, University of Maryland, College Park

L. J. LANZEROTTI

Bell Laboratories, Murray Hill, New Jersey

ELF-VLF (0.3-30 kHz) wave data measured at ground-based observatories for 250 sudden commencements were analyzed for amplitude and spectral modifications and correlated with magnetic field and precipitating particle observations. Changes in ELF-VLF wave activity at high-latitude stations were observed in 50-60% of the events studied and for approximately 80% of the events when the observing station was on the dayside. Characteristic, well-defined modifications of both coherent and incoherent ELF-VLF wave emissions were observed, including wave growth of the order of 20 dB, increases in the upper frequency limit of the waves, and enhanced triggering of discrete emissions. Wave growth generally occurred first at lower frequencies and with increasing delay at upper frequencies. The growth rate for the incoherent wave emissions (0.3-2.7 dB/s) was found to be at least 2 orders of magnitude less than known growth rates for coherent waves. Measurable particle precipitation inferred from cosmic noise signal absorption was observed to begin simultaneous to within 5 s of the wave growth onset in a significant number of cases, suggesting that at least a part of the observed precipitation results from wave-induced scattering.

1. INTRODUCTION

Observations have shown that sudden changes in the amplitude and spectrum of magnetospheric wave activity in the ULF, ELF, and VLF bands occur during sudden impulses (si) and sudden commencements (sc). The changes suggest that wave-particle interaction properties are significantly affected by the magnetic perturbation and plasma variations associated with si and sc. It is commonly believed that the interactions leading to the observed wave activity involve ion gyroresonance in the ULF band and electron gyroresonance in the ELF and VLF bands.

The occurrence of changes in wave activity during si has been well established, but the characteristic features, such as changes in the ELF-VLF amplitude and spectrum and the relation of ELF-VLF to particle precipitation, have not been carefully studied. *Morozumi* [1965] was the first to recognize that changes in ELF-VLF wave activity in the magnetosphere are associated with sc. *Hayashi et al.* [1968] examined several si and concluded that si were usually accompanied by abrupt changes in VLF chorus activity in the daytime and that positive/negative magnetic impulses were associated with increases/decreases in VLF noise. *Hayashi et al.* [1968] also noted that VLF emissions were always seen about 30 s prior to the magnetic perturbation at high latitudes and that the center frequency of chorus bands increased during positive si. These results led them to suggest that VLF wave growth rates along the dayside equator increase/decrease as a result of the magnetic compression/expansion. In their model, based on the gyroresonance theory of *Kennel and Petschek* [1966], the magnetic field change preferentially affects the perpendicular energy of gyrating electrons through betatron acceleration, changing the pitch angle anisotropy and thus modifying the growth rate. *Kokubun* [1983] suggested that betatron acceleration could provide an explanation for simultaneous VLF intensity enhancements and magnetic field changes which were observed during a several-hour period. *Korth et al.* [1985] used a recent refinement of the Kennel-Petschek theory by *Cornilleau-Wehrlin et al.* [1985] to explain wave activity observed by the GEOS 2 spacecraft during an sc. Work related to ULF phenomena [e.g., *Tepley and Wentworth*, 1962; *Kokubun and Oguti*, 1968; *Oguti and Kokubun*, 1969; *Hirasawa*, 1981; *Olson and Lee*, 1983] has indicated that ULF (0.1-1 Hz) emissions associated with si have spectral characteristics which are analagous to those of the ELF-VLF emissions. In addition, *Tepley and Wentworth* [1962] noted that the ULF emissions tend to be characterized by a transient amplitude enhancement lasting several minutes following the sc.

Observations of electron precipitation at the time of sc can be used to infer the existence and location of magnetospheric processes that drive the precipitation. *Brown et al.* [1961] first described ionospheric absorption and X ray production during an sc and suggested that they could result

[1] Now at the Aerospace Corporation, Los Angeles, California.
[2] Now at National Space Science Data Center, Greenbelt, MD 20771.

Copyright 1990 by the American Geophysical Union.

Paper number 89JA00623.
0148-0227/90/89JA-00623$05.00

from either precipitation of trapped particles or injection of particles from the solar wind. *Ortner et al.* [1962] and *Hartz* [1963] reported that ionospheric absorption during sc was localized around the maximum of the auroral zone, was rarely observed at geomagnetic latitudes below 57° or above 75°, and was most probable near local noon. They also noted that the absorption was generally limited to a duration of less than 15 min. Observations of X ray fluxes from balloon measurements near $L \simeq 6$ during an sc [*Ullaland et al.*, 1970] indicated periodicities of 1.8 s and 50 s in the observed particle precipitation during the event. *Leinbach et al.* [1970] found in a case study that absorption effects were similar at conjugate stations but that the time profile of the observed absorption depended on latitude. They concluded that precipitation of trapped electrons resulting from interactions with waves was the most probable cause.

In this paper we report on a study of ground-based observations which was undertaken to quantitatively characterize changes in ELF-VLF wave activity and ionospheric absorption associated with sc. In the companion paper [*Gail and Inan*, this issue] we describe similar observations of wave activity obtained with spacecraft. Waves observed at ground stations are generally believed to have propagated in magnetospheric ducts, while spacecraft instruments normally measure waves that are primarily nonducted. Ducted waves have small wave normal angles and propagate along field-aligned paths to their ionospheric exit points; nonducted waves may have a wide range of wave normal angles and can propagate across field lines. In addition to providing a descriptive model of the phenomenology of wave generation and particle scattering during sc, this set of papers is intended to establish an observational basis for understanding how wave-particle interactions in the magnetosphere are affected by dynamic variations in the magnetic field and plasma.

2. DESCRIPTION OF DATA SETS

Lists of sc were obtained from *J. Geophys. Res.*, *International Association of Geomagnetism and Aeronomy* 12 Bulletin (to 1969) and *No.* 32 (1970-1980), and *NOAA Solar-Geophysical Data* (1981-1985). Ground data for the study were obtained from several stations, which are listed in Table 1 along with geophysical and data set parameters. The Antarctic stations Palmer, Siple, and South Pole, which form a roughly meridional chain (collocated within ±1 hour geomagnetic local time with corrected geomagnetic latitudes of 48.5°, 61.1°, and 73.8°, respectively), were used to provide latitudinal comparisons. Magnetic local time (LT) at Palmer, Siple, and South Pole correspond to UT−4.5 hours, UT−5 hours, and UT−3.5 hours respectively (see Table 1).

ELF-VLF wave data were obtained with Stanford University receivers which have a bandwidth of 300 Hz to 20 kHz. Broadband data recorded on analog tape were generally available only for periods of 1 min out of every 5 or 15 min, although longer recordings were obtained for some events. Signals from the wave receivers as well as magnetometers and riometers were recorded in analog form on paper charts or in digital form with 1 sec resolution on University of Maryland digital data systems (depending on the station and year). Wave data were recorded as narrow-band amplitudes in the frequency ranges 0.5-1 kHz, 1-2 kHz, 2-4 kHz, 11-13 kHz, and 31-38 kHz.

TABLE 2. The Limited Set of sc Events Used for Detailed Analysis.

Year	Date	UT	Day
1982	Jan. 29	1744	029
1982	Feb. 5	1611	036
1982	March 1	1138	060
1982	April 1	1305	091
1982	April 16	1702	106
1982	June 12	1443	163
1982	July 16	1519	197
1982	Sept. 25	1703	268
1982	Oct. 31	1338	304
1982	Nov. 23	0917	327
1982	Nov. 24	0923	328
1983	Jan. 9	1544	009
1983	Feb. 4	1614	035
1983	April 12	1055	102
1983	April 13	1100	103
1983	Oct. 21	1324	294

Magnetometer data were obtained with the Bell Laboratories triaxial flux gate magnetometers which measure the magnetic field in the geomagnetic north-south (H), east-west (D), and vertical (Z) directions. The magnetometer noise level was $\simeq 0.2$ nT over the band dc to the Nyquist frequency in each component. The digitizer increment was equivalent to 0.06 nT. Riometer data were obtained with University of Maryland riometers at frequencies of 20.5

TABLE 1. Geophysical and Data Set Parameters for Ground Stations

Station	Geographic Latitude deg	Geographic Longitude deg	Geomagnetic Latitude deg	Geomagnetic noon UT	Data Set
Byrd (BY)	80.0 S	120.0 W	67.9 S	1800	1963-1965,1967-1968
Eights(EI)	75.2 S	77.2 W	59.5 S	1700	1963, 1965
Palmer A)	64.8 S	64.1 W	48.5 S	1630	1982-1983
Roberval (RO)	48.4 N	72.3 W	61.3 N	1700	
Siple (SI)	75.9 S	84.3 W	61.1 S	1700	1977-1978, 1982-1983
South Pole (SP)	90.0 S		73.8 S	1530	1981-1985

MHz, 30.0 MHz, and 51.4 MHz. Spacecraft magnetic field data were obtained with NOAA GOES satellites in geostationary orbit.

Approximately 250 sc from the period 1963 to 1985 were examined using the analog chart data during the preliminary portion of the study. Subsets of this data set were chosen for different types of analysis. Statistical results were based on data from South Pole, Siple, and Palmer during the period 1977 to 1985. A limited data set of 16 sc from the period 1982 to 1983 was used for much of the quantitative analysis; these events are listed in Table 2. A separate set of 6 sc was chosen for detailed ELF-VLF wave spectral analysis (the restriction to 6 sc was based on the availability of continuous broadband ELF-VLF wave data during the sc interval).

3. OBSERVATIONS

3.1. *Occurrence Statistics*

Statistical data on the occurrence of changes in wave activity associated with sc were compiled for South Pole, Siple, and Palmer covering the periods 1981-1985 at South Pole, 1977-1978 and 1982-1983 at Siple, and 1982-1983 at Palmer. Changes in wave activity were identified by examining amplitude plots from the narrow-band ELF-VLF filters for increases or decreases in wave amplitude within a few minutes of the time of the sc (see Figure 2 for examples). Events for which such changes could not be unambiguously differentiated from wave activity in the surrounding time period were identified as having no change. Histograms of the observed occurrence rates plotted versus universal time (UT) are shown in Figure 1. The number of reported sc during periods when data were available was 132 at South Pole, 104 at Siple, and 62 at Palmer. Distinct changes in wave amplitude in the narrow-band chart channels were observed in 67 of the cases at South Pole, 62 of the cases at Siple, and 22 of the cases at Palmer, corresponding to overall observation probabilities of 0.5, 0.6, and 0.3 respectively.

A broad maximum in occurrence rate of changes around geomagnetic noon (1530 UT) was noted at South Pole with a corresponding minimum near geomagnetic midnight (0330 UT). Occurrence rates as high as 0.8-1.0 were noted within several hours of local noon. A similar minimum near geomagnetic midnight occurred at Siple, but the distribution near noon was less peaked. Occurrence rates of 0.6-0.9 were observed at all local times except near midnight. At both stations, the occurrence rates near midnight were in the range 0.0-0.3. At Palmer, a maximum with occurrence rates of 0.3-0.6 was observed near local noon with a minimum observed near midnight. The occurrence statistics from Palmer are somewhat less reliable than the statistics for South Pole and Siple due to the smaller sample size.

Tsurutani et al. [1979] found no statistically significant longitudinal variation in the occurrence of natural ELF-VLF emissions, although there is some evidence for localized geographic dependence in particular regions such as the South Atlantic Anomaly. Consequently, the occurrence rate of 0.8 recorded at South Pole near local noon may be viewed as the probability that a station near local noon at the latitude of South Pole would observe emissions during any sc. This suggests that changes in ELF-VLF emissions observable at ground stations should occur during at least 80% of reported sc.

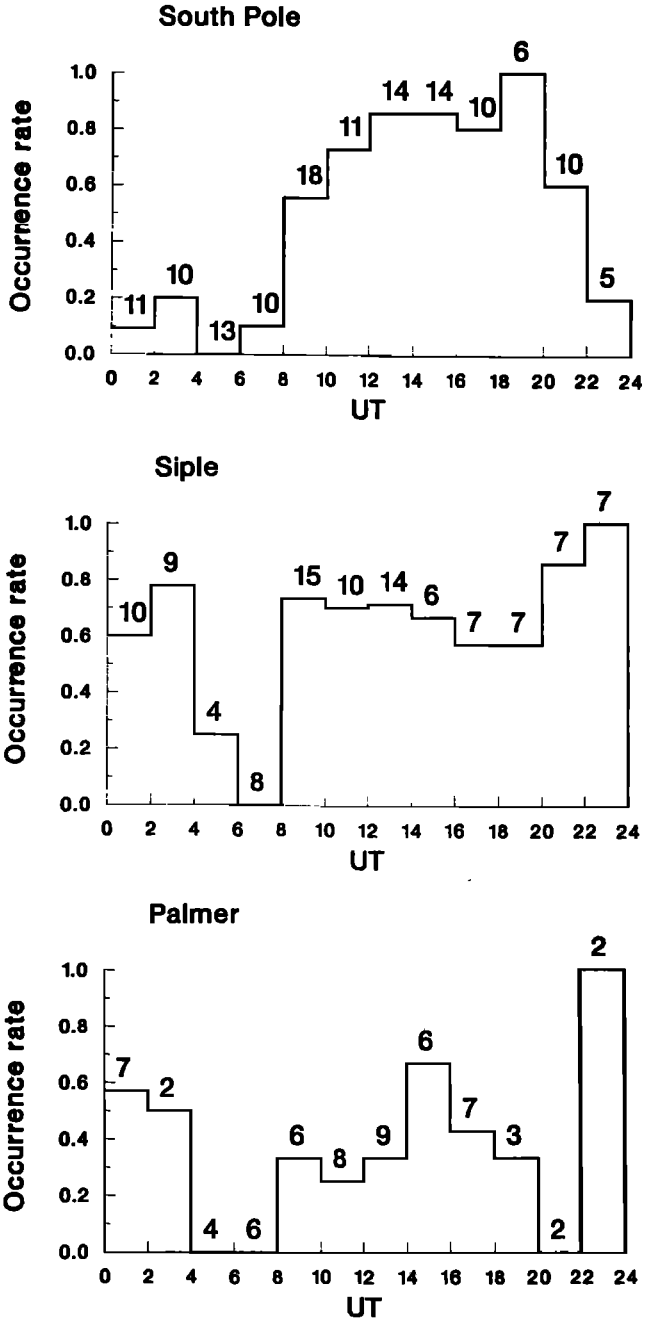

Fig. 1. Normalized occurrence rate of wave activity associated with sc at South Pole, Siple, and Palmer. Events are binned in 2-hour intervals and normalized by the total number of reported sc for which data were available (shown at the top of each bin).

3.2. *Wave Amplitude Characteristics*

Basic observations. Amplitude-time plots from South Pole for four of the limited data set of 16 sc are shown in Figure 2. Each panel shows the magnetic field H, D, and Z components as well as the ELF-VLF wave amplitudes in the bands 0.5-1 kHz, 1-2 kHz, and 2-4 kHz for a period of 1 hour, with times marked in UT. The impulse spaced at 5-min intervals in the ELF-VLF channels (e.g., Figure 2*c*) represent artificial calibration tones injected into the receiving system. The ELF-VLF channel amplitudes are uncalibrated, and the scale factors and zero levels of the linear displays have been adjusted for clarity in presentation.

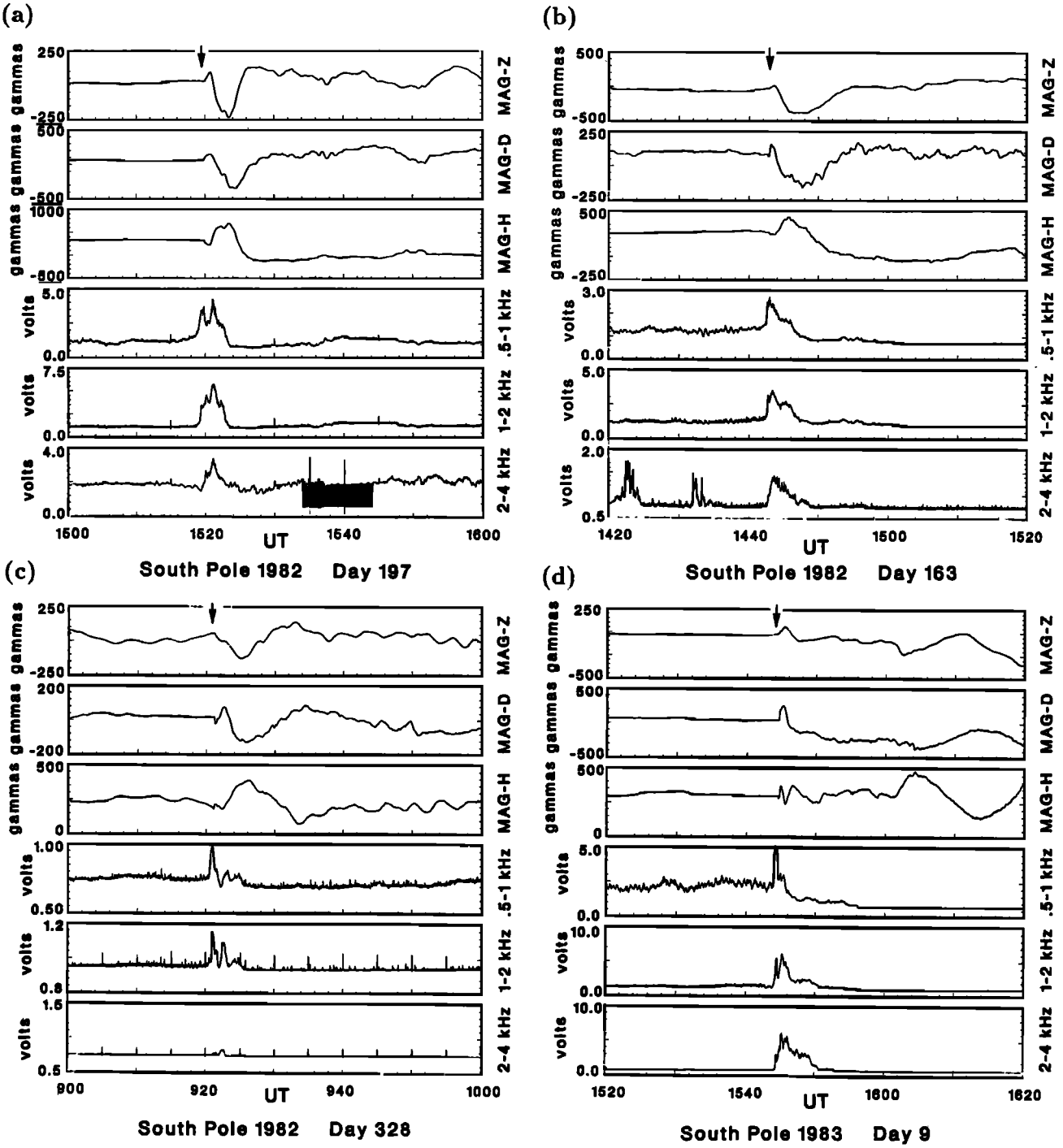

Fig. 2. Magnetic field and wave amplitude recorded at South Pole for four sc. Each panel shows the H, D, and Z components of the magnetic field and the ELF-VLF amplitude in the 0.5- to 1-kHz, 1- to 2-kHz, and 2- to 4-kHz channels. The periodic "spikes" in the ELF-VLF are calibration tones. The 2- to 4-kHz channel in Figure 2*a* does not accurately reflect the natural activity during this period as it was dominated by a subionospheric signal from the Siple transmitter.

In each example the onset of the sc was indicated by a sudden increase or decrease in the amplitude of the magnetic field components and was accompanied by distinct changes in the ELF-VLF amplitude in all three channels. Though both the 11- to 13-kHz and 31- to 38-kHz channels were also recorded during the 1982-1983 period, they rarely indicated amplitude changes associated with sc and thus are not included in the figures. The limitation of noise to the lower-frequency channels is consistent with the noise being primarily mid-latitude hiss, chorus, or polar chorus [*Helliwell*, 1965] rather than auroral hiss, in agreement with the observations of *Morozumi* [1965] and *Hayashi et al.* [1968]. Dynamic spectra for these events, which will be presented later in the section, confirm this conclusion.

Figure 2 shows four examples of sc observations at South Pole in which transient enhancements of wave activity lasting several minutes were observed (in Figure 2*a*, the amplitude of the 2- to 4-kHz channel does not accurately reflect the natural activity amplitude, since it was dominated by modulated or CW signals from the Siple transmitter at 3.8 kHz propagating subionospherically to South Pole). Each example shows that the wave amplitude increased for a period of 1-8 min at the time of the sc and subsequently returned to a steady level which differed from the original amplitude. The duration of the enhancement was dependent on frequency. The amplitude increase preceded the arrival of the magnetic perturbation at South Pole by up to 1 min. The growth time, defined loosely as the amount of time for the wave amplitude to increase from the preevent level to the first significant peak level, was 15-60 s for each channel in these events. The growth onset occurred first in the 0.5- to 1-kHz channel and with increasing delay in the 1- to 2-kHz and 2- to 4-kHz channels. A more complete analysis of the growth period using broadband data for several events is discussed in section 3.4.

Magnetic field — ELF-VLF correlation. Several authors [*Hayashi et al.*, 1968; *Korth et al.*, 1985] have suggested that wave amplitude increases/decreases are correlated with compression/decompression of the magnetic field. As indicated by Figure 2, the wave response to an sc is more complex than a simple increase or decrease of the wave amplitude.

In order to examine the magnetic field–wave relationship in more detail, the events in the limited data set were compared with the magnetic field at geostationary altitude recorded by the GOES satellites. In five of the six cases in which field strength increases were observed at GOES, the wave amplitude at South Pole was characterized by a several-minute transient increase followed by a decrease lasting several tens of minutes or longer. In the sixth case the wave amplitude was characterized by an increase lasting approximately 15 min. The duration of the transient enhancement, although clearly frequency dependent, was in most cases roughly comparable to the rise time of the magnetic disturbance at GOES. In both cases in which field strength decreases were observed at GOES, long-duration wave amplitude decreases were observed at South Pole. In one of the two cases in which a decrease was observed at GOES, an amplitude increase occurred in the 2- to 4-kHz channel at Siple. In spite of the clear correlation between the onset of the magnetic perturbation and changes in the wave activity, the correlation between the subsequent ground/satellite magnetic field signatures and further wave activity in each case was not obvious.

Wave amplitude oscillations. Periodicities in the data were analyzed by using a high-pass filtered to eliminate oscillations with periods smaller than 10 s. Well-defined oscillations in the wave amplitude were observed during the transient wave enhancement in several events. In 12 of the 16 events in the limited data set, 3-4 cycles of a damped oscillation with period 60-90 s were observed in the ELF-VLF channels. The extent of the correlation between the oscillations in the magnetic field and the wave amplitude is not clear, however. Oscillations with periods in the range 60-90 s were apparent in the magnetic field at South Pole as well as in the wave amplitude in at least eight of the cases when the data were high-pass filtered to emphasize the oscillations. However, the magnetic field oscillations did not have the damped structure observed in the wave amplitude, and in most of the eight cases there was a small but measurable difference (typically 10-20%) between the magnetic field and wave periods. In two of the events studied the 0.5- to 1-kHz and 1- 2-kHz channels showed clear fluctuations of approximately the same period prior to the sc, suggesting the possibility that the oscillations associated with the sc represented a fundamental periodicity of the system independent of the sc-induced perturbation.

A possible explanation for the oscillations is an oscillatory modulation of the magnetoplasma superimposed on the sc compression. *Baumjohann et al.* [1983] found 2-min oscillations in both the plasma drift and the magnetic field at the GEOS 2 spacecraft during an sc and attributed them to an overshoot and subsequent oscillation of the magnetopause velocity about the expected value. The 2-min periods are slightly longer than the observed ELF-VLF periods of 60-90 s. A number of investigators have reported damped magnetic oscillations with fundamental periods typically 4-5 min both on the ground [e.g., *Wilson and Sugiura*, 1961] and at spacecraft altitudes [*Barfield and Coleman*, 1970; *Baumjohann et al.*, 1984] as well as apparent harmonics starting near 40 s [*Fukunishi*, 1979; *Sakurai et al.*, 1984; *Wedeken et al.*, 1986]. Such oscillations are often attributed to field line resonance. The fundamental periods tend to be somewhat longer than the ELF-VLF periods, but the harmonic periods are in the correct range. The similarity of the ELF-VLF and magnetic field oscillation periods at South Pole supports the relation between magnetic field and wave activity. The lack of one-to-one correlations, however, limits conclusions regarding an intervening mechanism. Another possible explanation of the oscillations is that the transient response of the wave growth rate to the steplike magnetic perturbation results in an overshoot and subsequent oscillation of the wave amplitude about the equilibrium level. The oscillation period would be a function of the wave-particle interaction time scales (e.g., diffusion time, drift rate) but would probably be independent of the magnetic field driving function. This explanation is consistent with the observation of oscillations prior to as well as after the sc.

3.3. *ELF-VLF Wave Spectral Characteristics*

Synoptic dynamic spectra. The relative rarity of sc and the multiminute duration of the wave response makes it difficult to obtain continuous broadband data for the full duration of an sc. For most cases studied here, broadband data were available only at the synoptic intervals of 1 min in every 5 or 15 min. Figure 3 shows dynamic spectra from synoptic recordings for each of the events illustrated in Figure 2. The figures illustrate a number of long-term changes in ELF-VLF spectra commonly observed during sc. Spectrograms are shown for the band 0-4 kHz or 0-5 kHz for three 10-s periods with samples separated in time by 15 min. For each event, spectrograms from South Pole, Siple (or Roberval), and Palmer are included for intervals prior to, during, and after the sc whenever possible. The samples can be compared with the corresponding amplitude records to determine the extent to which each sample represents typical wave activity for the corresponding period. Some of the features of the spectrograms result from terrestrial interference effects. The vertical lines are due to atmospherics (sferics) from lightning, and the noise band below 400 Hz,

which appears to consist of impulsive emissions, is also due to sferics. The nearly monochromatic lines seen mostly at lower frequencies are power line harmonics from the local power distribution systems. In the following discussion the approximate upper and lower cutoff frequencies of the observed wave activity will be referred to as the UCF and LCF, respectively.

In each of the examples, the first sample shows that polar chorus consisting of diffuse and discrete emissions with a UCF in the range 0.5-2.5 kHz was observed prior to the sc at South Pole. In eight of the 16 examples (e.g., Figures 3*a*, 3*b* and 3*d*), data from Siple/Roberval were available and showed similar polar chorus activity with a UCF within a few hundred hertz of that observed at South Pole, although differences in band structure and LCF were apparent. In three of the eight cases (e.g., Figure 3*b*), similar discrete emissions were identifiable in the spectrograms from South Pole and Siple after the sc, indicating that both stations were observing wave activity from the same source region. In Figure 3*b*, in spite of the clear correlation between discrete emissions, the LCF at Siple was significantly higher than that at South Pole. Differences in the subionospheric propagation losses between the ionospheric exit point of the wave activity and the two receivers may account for such differences, or South Pole may have been observing an additional source region not observed at Siple. In four of the 16 examples (e.g., Figure 3*c*), wave activity observed at Siple prior to the sc was distinctly different from that observed at South Pole.

The second sample in each example shows the wave spectrum during or immediately after the sc. Comparison with the first samples shows the changes that occurred in the ELF-VLF signals due to the sc. In Figures 3*a*, 3*c* and 3*d*, the second sample includes some portion of the transient wave enhancement associated with the first few minutes after the onset of the sc. In each case an increase in the UCF was observed at both South Pole and Siple/Roberval (when available), in several cases by as much as 1 kHz or more. Five of the cases showed an increase in the LCF as well, as is evident in Figures 3*a*, 3*b* and 3*d*. In general, both the diffuse and discrete emissions components of the observed wave spectra were modified following the sc. In Figure 3*d*, well-defined discrete emissions are evident near the new UCF at Siple with no comparable emissions apparent in the South Pole data, in spite of the fact that similar emissions occurred at both stations prior to the sc.

The third sample represents the long-term (order of ~10 min after the sc) modification of the wave spectrum associated with each event. In each case the spectrum in the third sample was distinctly different from that in the first sample, suggesting that modifications of the wave source were not simply transient. The long-term modifications varied considerably among events. In Figures 3*a*-3*d*, decreases in the amplitude of the diffuse emissions and the occurrence rate of discrete emissions were observed. Distinct amplitude increases and corresponding modifications of the bandwidth and spectral structure were observed in other events.

In only one of the 16 events (Figure 3*a*) did Palmer ($L \sim 2.3$) record a change in wave activity associated with the sc. In this case, Palmer observed very little wave activity prior to the sc. During the transient enhancement, diffuse emissions in the band 0-3 kHz with some evidence of discrete (and periodic) structure were observed. Following the transient enhancement, the wave activity was similar to that prior to the sc.

Continuous dynamic spectra. For the limited data set, continuous data were available for only one event (that of Figure 2*a*). A dynamic spectrogram for the event is shown in Figure 4*a*. This event provides a good illustration of the initial amplitude enhancement as well as the long-term spectral modification. Prior to the onset of wave growth near 1519 UT, the spectrum consisted of a diffuse emissions band with LCF below 100 Hz, UCF at approximately 0.8 kHz, and a band of discrete emissions from the UCF of the diffuse emissions to about 1.4 kHz (spectral features such as discrete emissions may be more apparent in the higher-resolution spectrograms for four of these events shown in Figures 6-9). At the time of the sc the UCF of the diffuse noise began to increase, reaching 2.2 kHz after 30 s and remaining near this frequency for about 3 min. No similar increase was noted in the UCF of the discrete emissions, which disappeared entirely starting at the time of the transient enhancement (during the transient enhancement this may have been due simply to an inability to distinguish them from the diffuse emissions). An increase in the LCF to about 300 Hz was also observed. The UCF of the diffuse noise subsequently decreased to 300 Hz, and the discrete emissions became sporadic. The growth onset period will be discussed in more detail in section 3.5.

Figures 4*b*-4*d* and Figure 5 show dynamic spectra for six other events for which continuous broadband data were available at the time of the sc (including data from both Byrd and Eights for one event). In each case a transient enhancement of the wave activity was observed together with an increase in the UCF. The length of the transient amplitude increase varied from 1 to 6 min, and the corresponding rise time of the UCF varied from less than 1 min to several minutes. In all examples except Figure 4*c*, the wave activity consisted primarily of a diffuse component with discrete emissions that occurred primarily near the UCF of the diffuse emissions. In Figure 4*c*, only discrete emissions were observed, and a clear increase in both the frequency range and the UCF of the emissions was observed following the sc.

3.4. *Wave Growth Characteristics*

Basic observations. The initial wave growth period, in most cases the first several tens of seconds of the event, provides the best opportunity for making measurements which can be compared with theoretical predictions. For this study the growth period was examined in detail for six sc (data from both Byrd and Eights were available for one sc). Dynamic spectra for each of the events are shown in Figures 4 and 5. Measured values for the initial and final UCF, onset delay between lowest and highest frequencies, total wideband growth amplitude, narrow-band growth rate and growth duration, maximum narrow-band growth amplitude, growth bandwidth and center frequency, and dynamic range of the growth band prior to the sc are listed in Table 3 for the six events.

Figures 6-9 illustrate four examples of wave activity during the wave growth period of the sc. The data for the

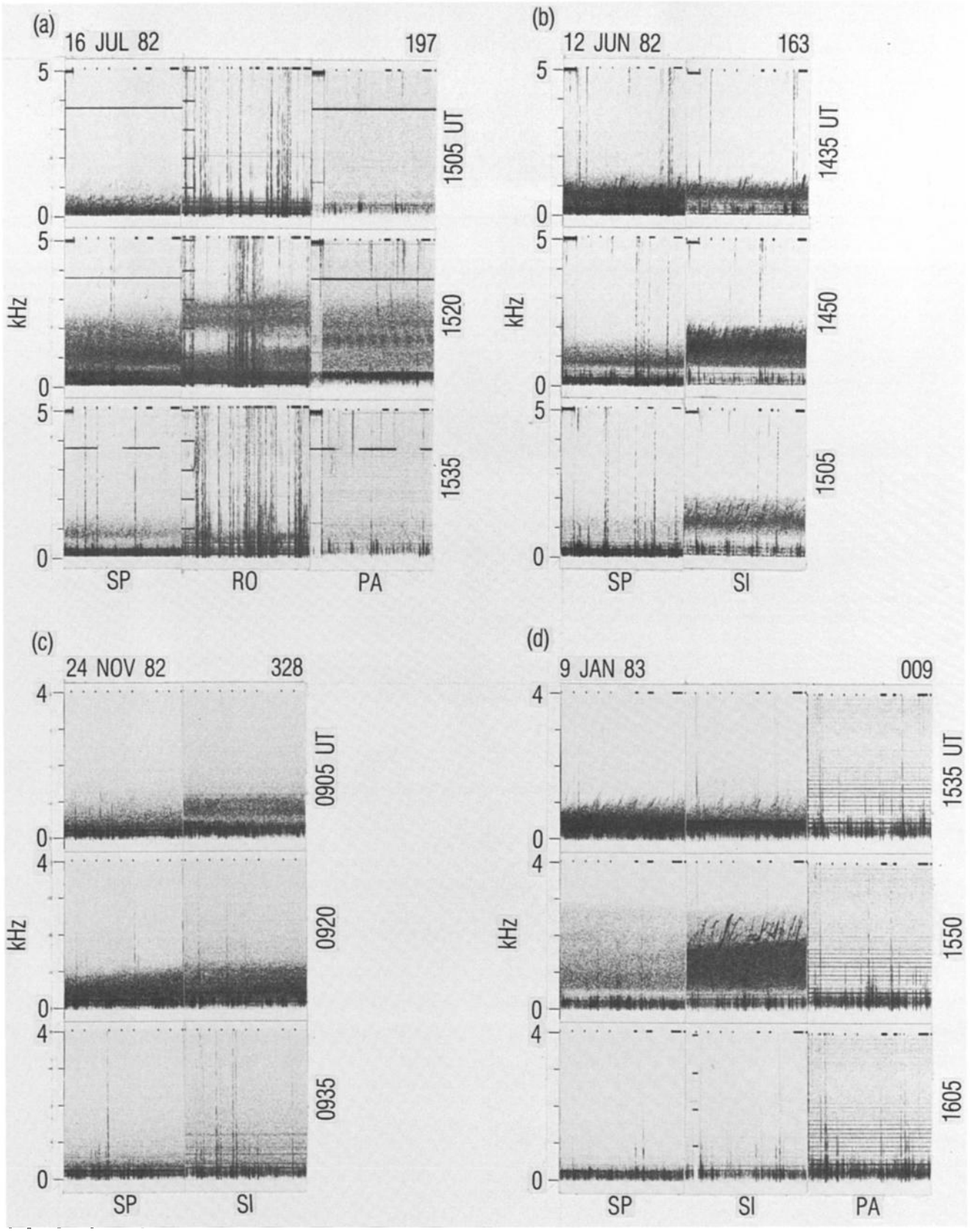

Fig. 3. Synoptic dynamic spectra recorded at South Pole, Siple, and Palmer for four sc. Each panel shows dynamic spectra in the band 0-4 or 0-5 kHz for three 10-s periods separated in time by 15 min. The periods were chosen to illustrate the spectra prior to, during, and after the sc whenever possible.

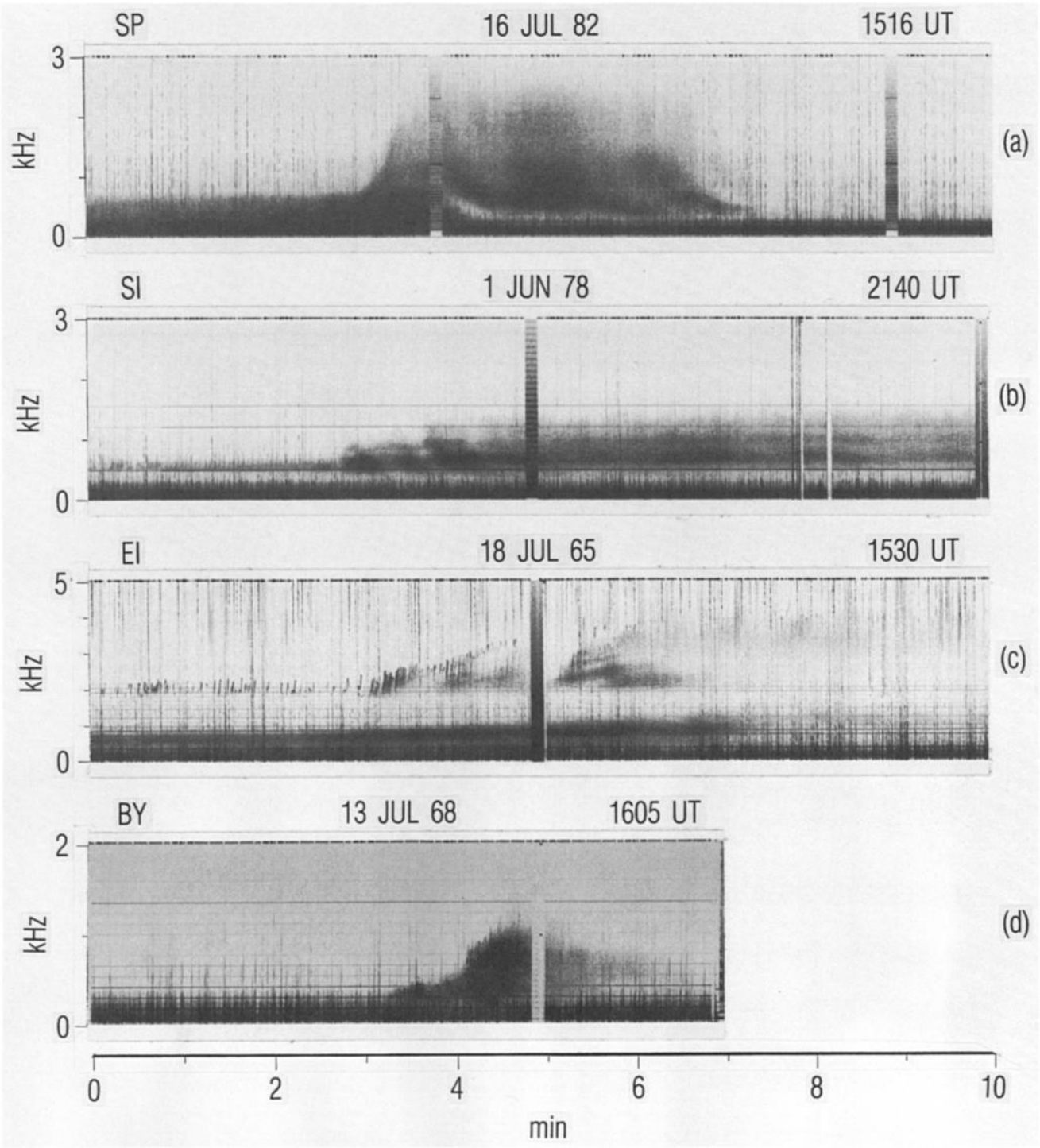

Fig. 4. Continuous dynamic spectra for four sc. The figure illustrates the transient wave enhancement commonly observed during sc.

figures were digitized from the original broadband analog tapes and processed in digital form. In each example the top panel is a dynamic spectrogram showing the changes in the wave spectrum observed during the growth period. The time scale shows elapsed seconds starting from the time shown at the top of the plot. The bottom panel shows the amplitude in a number of narrow-band channels corresponding to the period shown in the spectrogram. The 0-dB reference level is the same for both the spectrogram and the amplitude plot. The bandwidth of the narrow-band filters was 50 Hz. The filter output was low passed, in order to distinguish the growth trend from higher-frequency fluctuations in the wave amplitude, and processed to remove the impulses caused by sferics. The filter center frequencies are indicated by the legend on the right-hand side of the plot. In each of the figures, however, amplitude generally decreases with frequency so that the figure can be viewed in a simple manner by recognizing that the center frequency of the filter channels increases as the plot is scanned downward.

The upper cutoff frequency. As noted previously, the UCF increases during the growth phase with growth observed first at lower frequencies and with increasing delay at higher frequencies. The increase was a factor of 1.3-2.8 times the initial UCF for these events, corresponding to a frequency

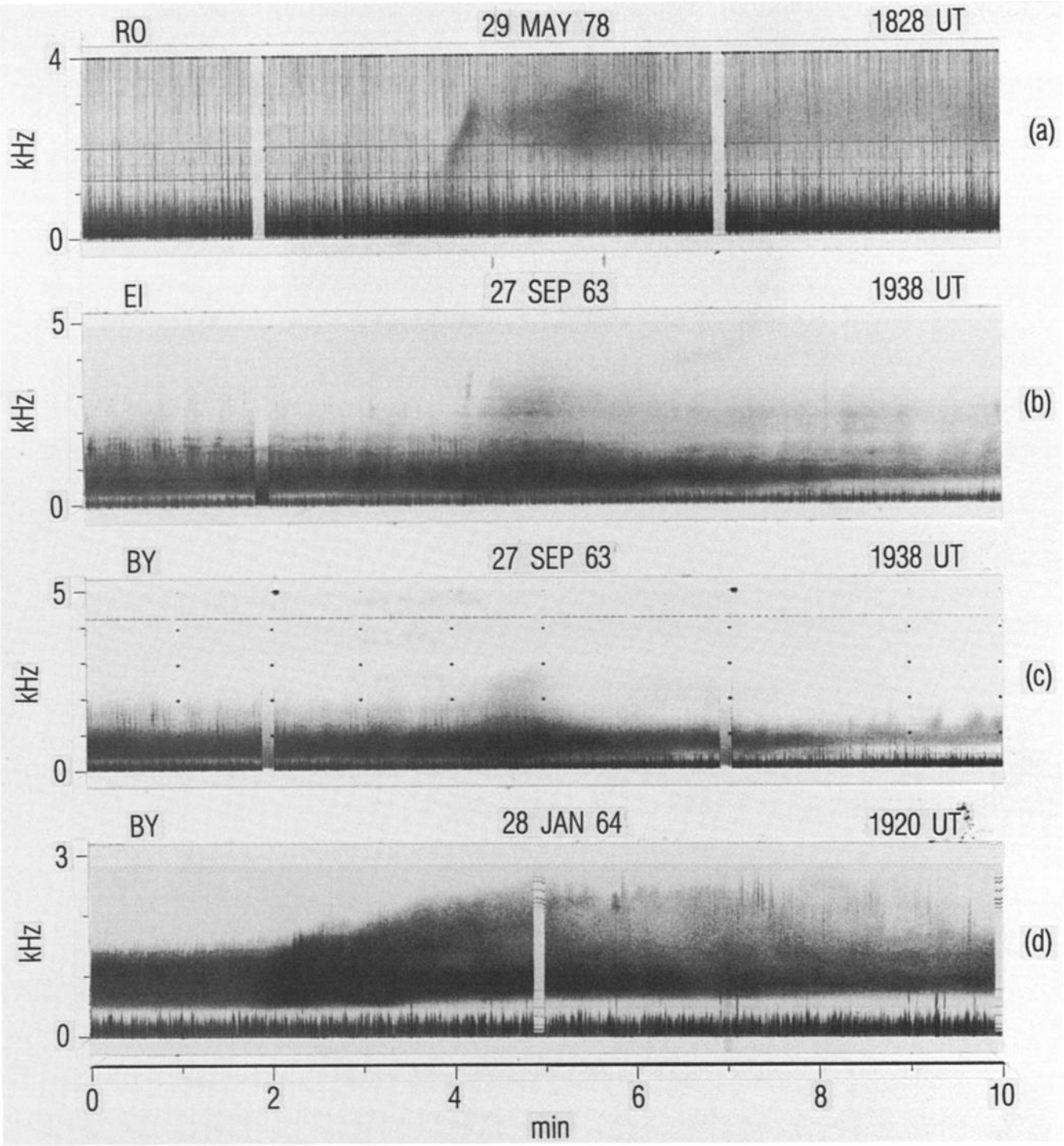

Fig. 5. Continuous dynamic spectra for four sc. The figure illustrates the transient wave enhancement commonly observed during sc.

increase of 0.3-1.4 kHz. The delay between the growth onset at lower frequencies and at higher frequencies was 10-35 s.

Narrow-band measurements. The maximum total narrow-band growth varied from 12 dB to 29 dB in the seven examples. Defining the growth bandwidth as the frequency range for which the total growth was within 3 dB of the maximum total growth, the growth bandwidth for the events was 0.4-1.2 kHz. The narrow-band growth rates within the growth band were within the range 0.3-2.7 dB/s and were roughly constant over the 3-dB bandwidth. The growth rate and total growth at a given frequency showed no dependence on the initial wave amplitude. These features are particularly evident in Figure 6, for which growth rate and total growth were roughly constant over a bandwidth of 1.2 kHz and an initial dynamic range of 20 dB.

Total growth. The total growth integrated over the entire growth band (for this measurement, all frequencies for which growth was observed were included in the filter band) is shown in Figure 10 for each of the events. Total integrated growth for the events ranged from 5 dB to 20 dB with growth times of 20-45 s.

Multiple station observations. The sc on September 27, 1963 (Figure 5) is of particular interest because data are available which show the growth period for one event

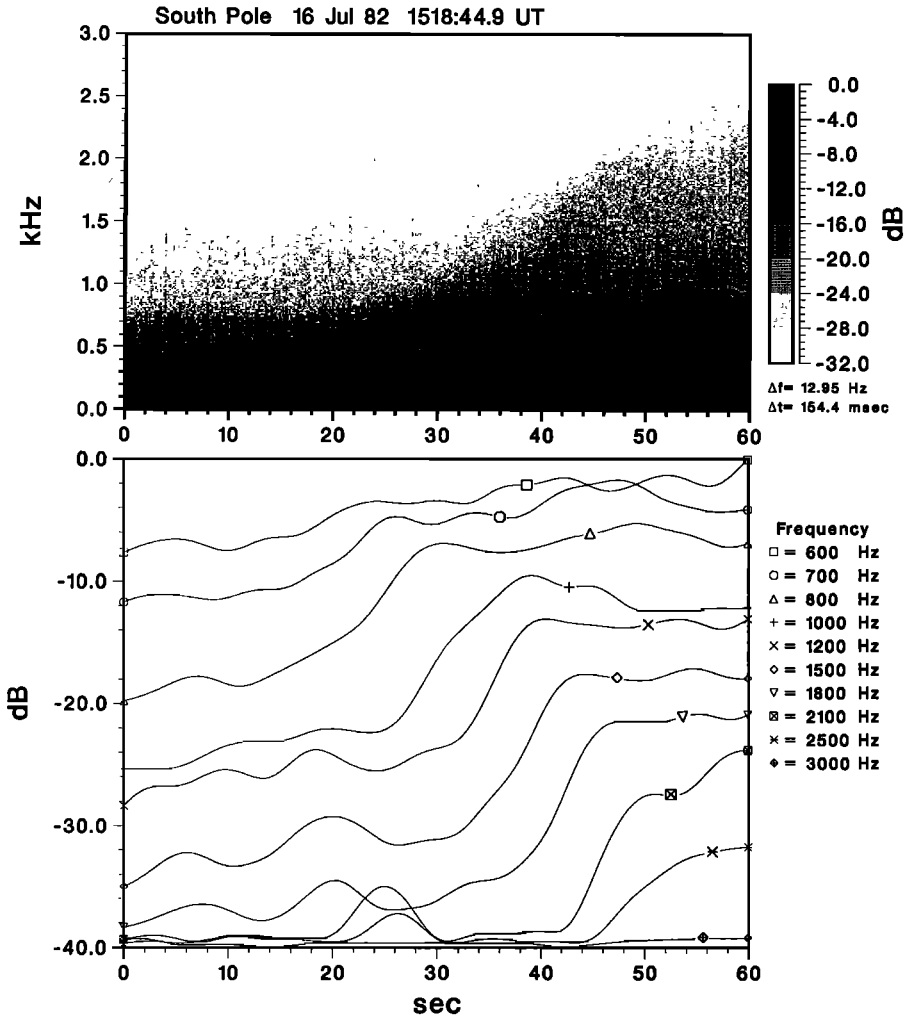

Fig. 6. Dynamic spectra and narrow-band amplitude plots for the wave growth period. The top panel shows dynamic spectra for the period during which wave growth was observed. The bottom panel shows amplitude in a number of narrow-band channels for the same period.

recorded at two stations, in this case Byrd ($L \sim 7$) and Eights ($L \sim 4.1$). Total growth and growth time were approximately equivalent at both stations. The UCF was approximately 0.3-0.4 kHz higher at Eights than at Byrd both prior to and after the sc. Both stations observed an increase of 1.1-1.2 kHz in the UCF. The onset of the growth phase appears to have occurred at about 55 ± 10 s at each station. The maximum total narrow-band growth was the same (13-14 dB) at both stations. Thus the two stations appear to have observed very similar phenomena during this event.

TABLE 3. Measured Values for Growth Phase Characteristics.

Event	Initial UCF, kHz	Final UCF, kHz	Onset Delay s	Wide-band Growth, dB	3-dB Growth Rate, dB/s	3-dB Growth Time, s	3-dB Maximum Growth, dB	Band-width, kHz	Center Frequency, kHz	Dynamic Range, dB
July 16,1982 SP	0.8	2.2	30	10	1.3-1.8	8-14	16	1.2	1.5	20
July 13,1968 BY	0.4	1.1	35	20			29	0.4	0.8	7
May 29,1980 RO		3.3	10	6	1.5-2.5	9-14	12	1.2	2.4	2
June 1,1978 SI	0.7	1.0	10	6	1.3-2.7	8-16	14	0.5	0.9	17
Jan.28,1964 BY	1.4	1.8	35	5	1.5-1.3	10-30	14	0.5	1.5	14
Sept.27,1963 BY	2.4	3.5	20	5	0.3-0.4	20-30	13	1.2	2.9	13
Sept.27,1963 EI	2.7	3.9	20	5	1.3-2.0	10-20	14	1.2	3.1	13

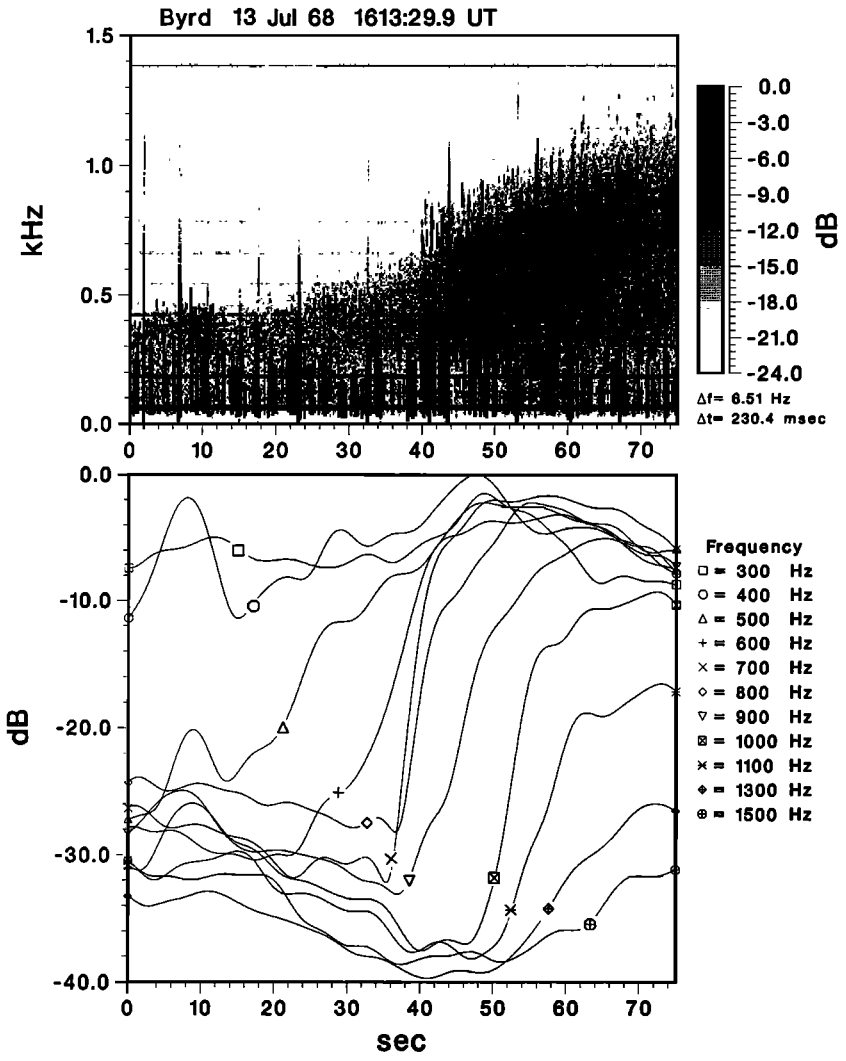

Fig. 7. Dynamic spectra and narrow-band amplitude plots for the wave growth period. The top panel shows dynamic spectra for the period during which wave growth was observed. The bottom panel shows amplitude in a number of narrow-band channels for the same period.

3.5. *ELF-VLF Wave Growth Onset Time*

Since it is possible to make accurate measurements of the arrival time of both the whistler mode waves and the magnetic disturbance on the ground as well as the magnetic disturbance at spacecraft locations, the measurements may be used to help identify the wave source region. This technique was first suggested by *Hayashi et al.* [1968], who proposed that the approximately 30-s delay they observed between the arrival of the waves and the magnetic disturbance represented a propagation time difference between the waves traveling at the whistler mode group velocity and the magnetic disturbance propagating at the much smaller Alfvén velocity from a source region in the equatorial plane. For this analysis, events were chosen for which both the wave and magnetic perturbation onset could be determined from the University of Maryland South Pole digital data to within an estimated accuracy of ±10 s or better. The GOES magnetometer data were measured to an estimated accuracy of ±5 s. The errors are in general significantly larger than the sampling period and reflect a subjective determination of the accuracy with which a particular onset can be identified. The error bars in the data plots refer to these measurement errors. These measurements will be discussed further in section 4 in an effort to determine the location and extent of the wave generation regions associated with sc.

ELF-VLF wave growth/ground magnetic field delay. Figure 11*a* shows the measured delay between the arrival of the waves and the magnetic perturbation plotted versus the magnetic local time of South Pole. Positive delays indicate that the magnetic perturbation arrived after the wave onset. The delays had a mean value of 30 s and a standard deviation of 18 s. Although the delays were almost exclusively within the range 0-60 s, there was no strong tendency toward any single value nor an obvious dependence on local time. The observed variations are much larger than would be reasonable to expect from the measurement errors. These observations suggest that if the explanation proposed by *Hayashi et al.* [1968] is correct, differences in Alfvén velocity or location of the wave source region from case to case add variability in the delay of the order of the measured standard deviation in the data. In individual cases, such variability complicates the use of delay measurements at single locations to identify the source region.

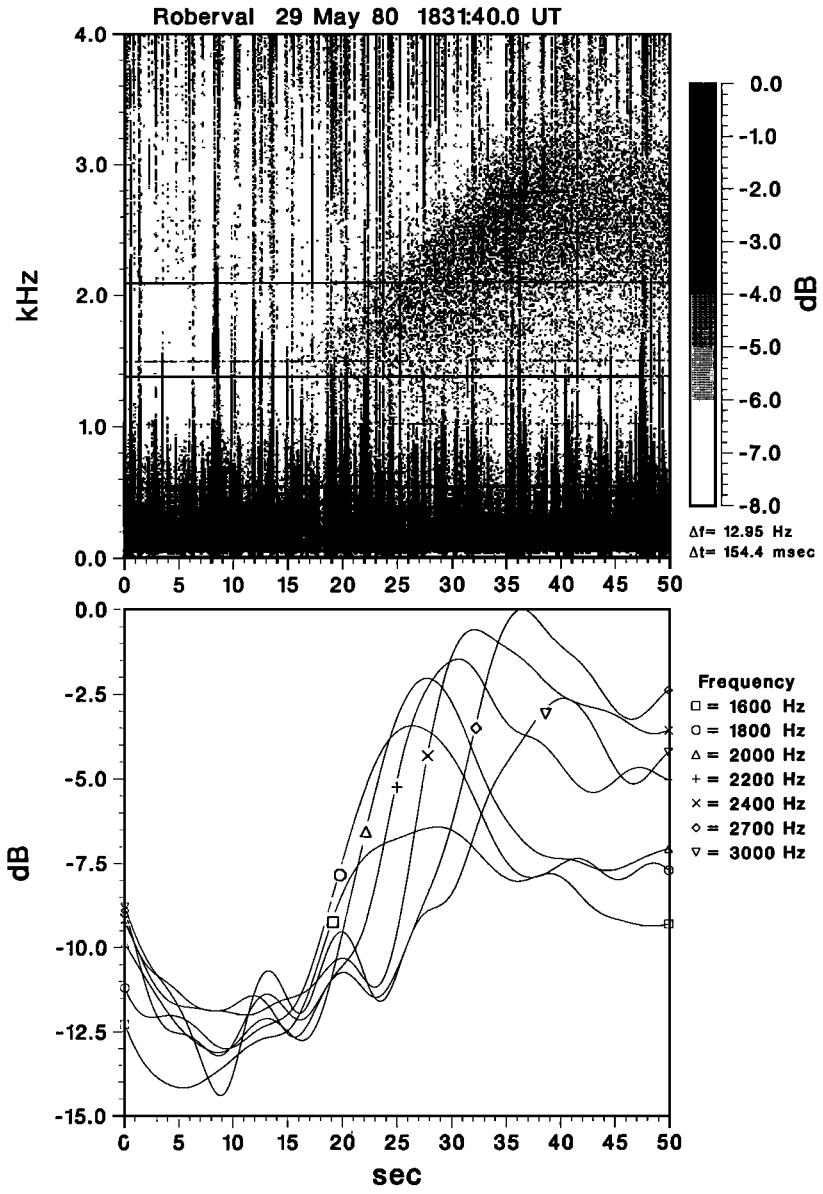

Fig. 8. Dynamic spectra and narrow-band amplitude plots for the wave growth period. The top panel shows dynamic spectra for the period during which wave growth was observed. The bottom panel shows amplitude in a number of narrow-band channels for the same period.

ELF-VLF wave growth/GOES magnetic field delay. Figure 11(b) shows the measured delay between the arrival of the waves on the ground and the onset of the magnetic disturbance at GOES plotted versus the local time at GOES. The figure shows a clear dependence of the delay on local time with apparent minimum and maximum values of 10±20 s at noon and 100±20 s at midnight. Such a delay could have a number of causes, but it should be noted that 120 s is approximately the delay time for the sc disturbance to propagate from noon to midnight at geostationary altitudes, as can be inferred from the results of *Kuwashima and Fukunishi* [1985]. The variation in the delays is again significantly larger than the measurement errors.

3.6. *Particle Precipitation Characteristics*

Numerous investigators have studied particle precipitation during sc using riometer observations. In this section, riometer data from the University of Maryland riometer systems at South Pole and Siple are presented for the events in the limited data set.

The output of the 20.5-, 30.0-, and 51.4-MHz riometer channels along with the corresponding magnetic field H component and 0.5- to1-kHz amplitude at South Pole are shown for four events from the limited data set in Figure 12. Each channel was low-pass filtered to remove high-frequency fluctuations. Each plot covers an interval of 10 min. The dashed line indicates the time when the onset of wave growth was observed. The pre-sc absorption level was measured just prior to the increase in riometer absorption. The post-sc level was measured at the first distinct maximum, in the absorption. In half of the events the absorption continued to increase after the first distinct maximum, and an overall maximum was reached typically several tens of minutes after the absorption onset (not shown in these figures). The

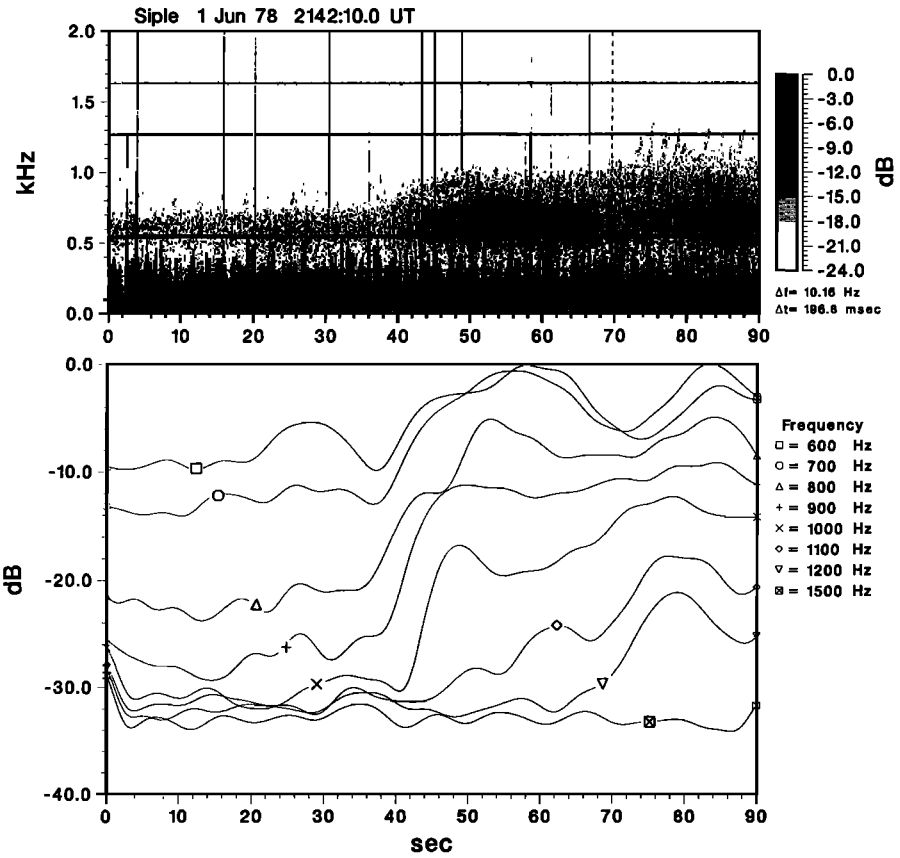

Fig. 9. Dynamic spectra and narrow-band amplitude plots for the wave growth period. The top panel shows dynamic spectra for the period during which wave growth was observed. The bottom panel shows amplitude in a number of narrow-band channels for the same period.

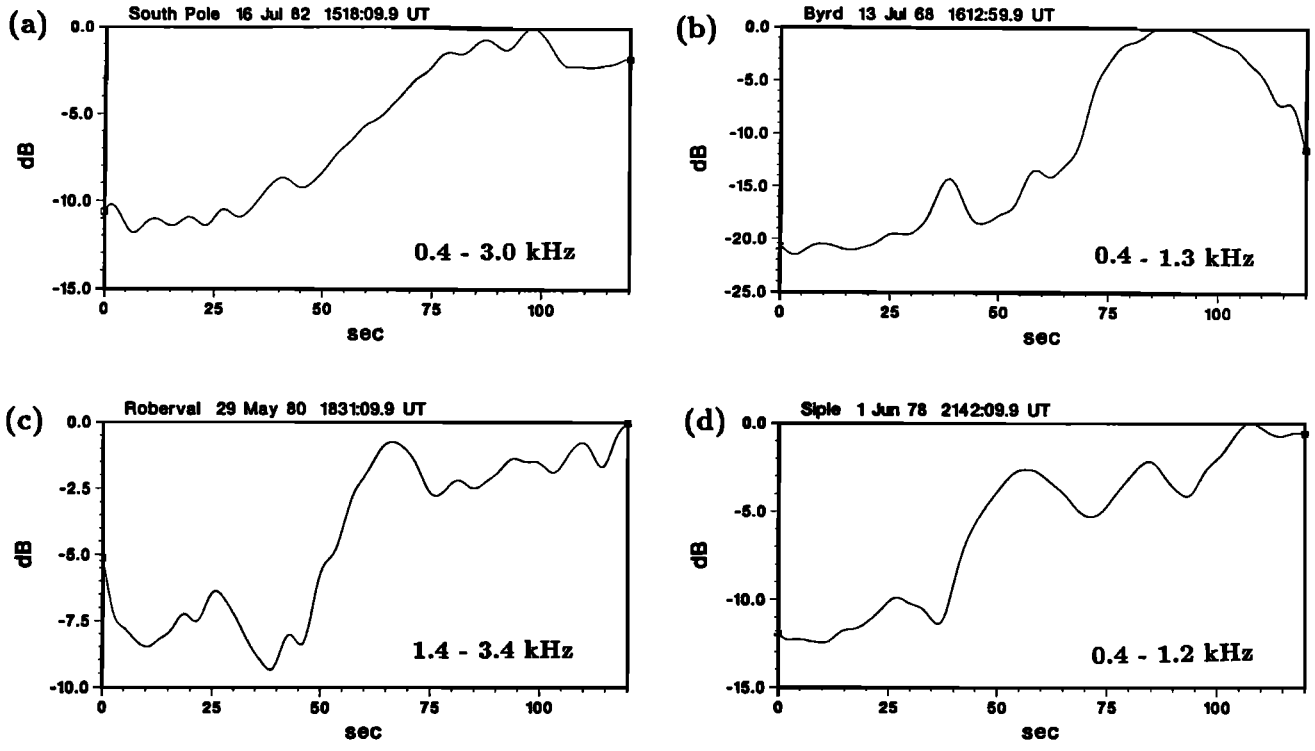

Fig. 10. Wideband amplitude plots for the wave growth period. The filter pass bands were chosen to include all magnetospheric wave energy and exclude the sferic wave energy at lower frequencies.

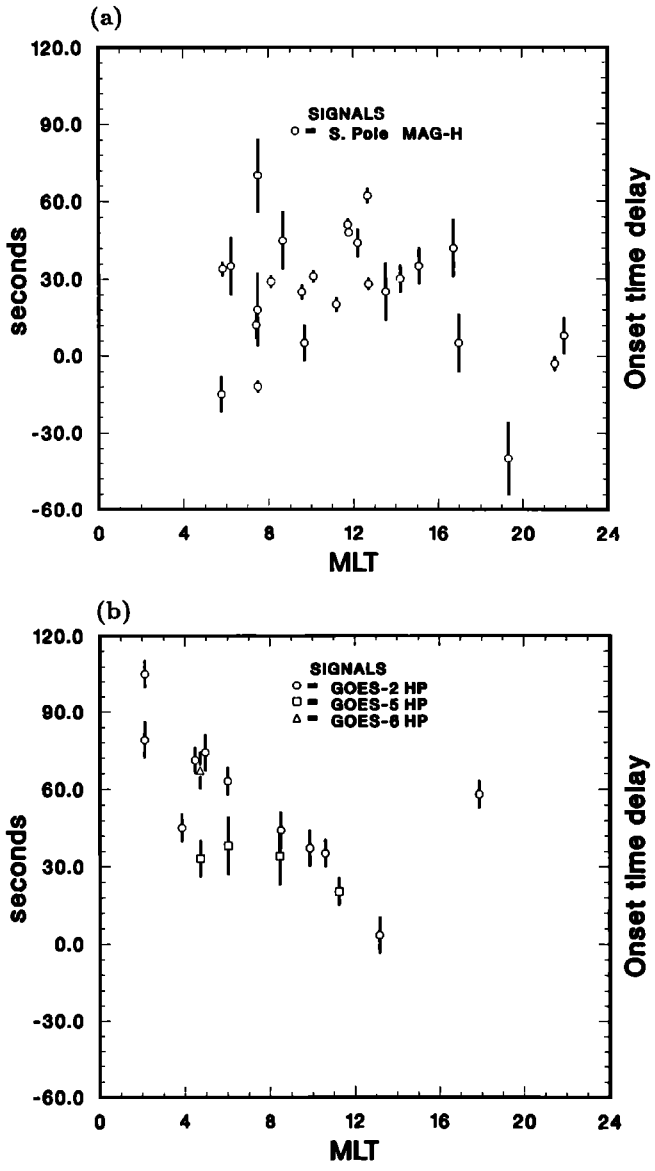

Fig. 11. Measured delay between the onset of wave growth and the magnetic disturbance. (*a*) The delay between the onset of ELF-VLF wave growth and the arrival of the magnetic disturbance at South Pole. (*b*) The delay between the onset of wave growth at South Pole and the arrival of the magnetic disturbance at the GOES spacecraft.

earlier maximum was chosen to best represent the initial absorption due to precipitation associated with the transient wave enhancement and to eliminate possible contributions from subsequent storm effects. The typical measurement error was estimated to be ±0.05 dB.

Absorption values. Of the 16 events 12 showed riometer absorption that was clearly associated with the sc (e.g., Figures 12*a*-12*d*). In 8 of the 16 events, a background absorption level greater than 0.1 dB at 30 MHz was present prior to the sc. Typical sc absorption values, with the background level subtracted, were 0.2-1.0 dB at 20.5 MHz, 0.1-0.4 dB at 30.0 MHz, and 0.0-0.2 dB at 51.4 MHz.

Absorption onset timing. In five of the events (e.g., Figures 12*a* to 12*c*), the onset of both the ELF-VLF wave growth and the riometer absorption could be identified quite clearly and appeared to be coincident within a measurement error of ±5 s. In four other events (e.g., Figure 12*d*), there is some indication that riometer absorption may have begun coincident with the wave growth onset, but the signal was too noisy to make a positive identification. In the five most well-defined cases the time delay between the onset of riometer absorption and the arrival of the magnetic perturbation at South Pole was 20-50 s. The onset of the riometer absorption clearly preceded the arrival of the magnetic perturbation in most of the cases.

Absorption structure. As shown in Figure 12, the first absorption maximum typically occurred 2-3 min after the absorption onset, a time period comparable to the length of the transient ELF-VLF wave enhancement. Absorption generally continued for a period somewhat longer than that of the transient enhancement, however. In 10 of the 16 cases, absorption continued for 30 min or longer.

4. DISCUSSION

The compression of the magnetosphere during an sc causes the dipolar geomagnetic field lines to move earthward, as shown schematically in Figure 13. For the particle energies of interest, the azimuthal drift velocities are sufficiently small that both thermal and energetic particles are effectively "tied" to a given field line throughout the sc compression, violating the third adiabatic invariant [e.g., *Schulz and Lanzerotti*, 1974]. A duct, which is a field-aligned enhancement of thermal plasma, thus remains collocated with a given field line, and both the waves and particles associated with a particular duct prior to the sc will be associated with that duct throughout the sc. In order to interpret the observations, we need to understand how to translate ground-based measurements (e.g., growth rate) into parameter values that would be valid within the interaction region. Ground-based wave receivers measure a signal which has undergone an integrated growth process along the length of a duct. The signal may be composed of contributions from several source regions; each contribution will have been modified by propagation between the source and the receiver, so that the importance of both source location and propagation effects must be discussed.

4.1. Location of Source Regions

The sc disturbance originates near the subsolar point on the magnetopause and propagates as a compressional wave at the local Alfvén speed throughout the entire inner magnetosphere within several minutes. Presumably, changes in wave activity occur with some local time and radial dependence as a result of the sc perturbation. It is thus desirable to know the location and extent of wave source regions and their relative contribution to the signal observed on the ground. Ground-based ELF-VLF wave receivers suffer, in this instance, from their large viewing area (500-1000 km [*Walker*, 1974; *Tsuruda et al.*, 1982]), which limits the degree to which wave observations can be related to source regions. There are, however, a number of techniques that can be used to address the problem.

Onset time measurements. A simple estimate of the location of the source region for the earliest wave growth observed on the ground can be made using the onset time measurements described in section 3.5. The arrival of the magnetic perturbation at geostationary altitudes is known to be strongly local time dependent (corresponding to the

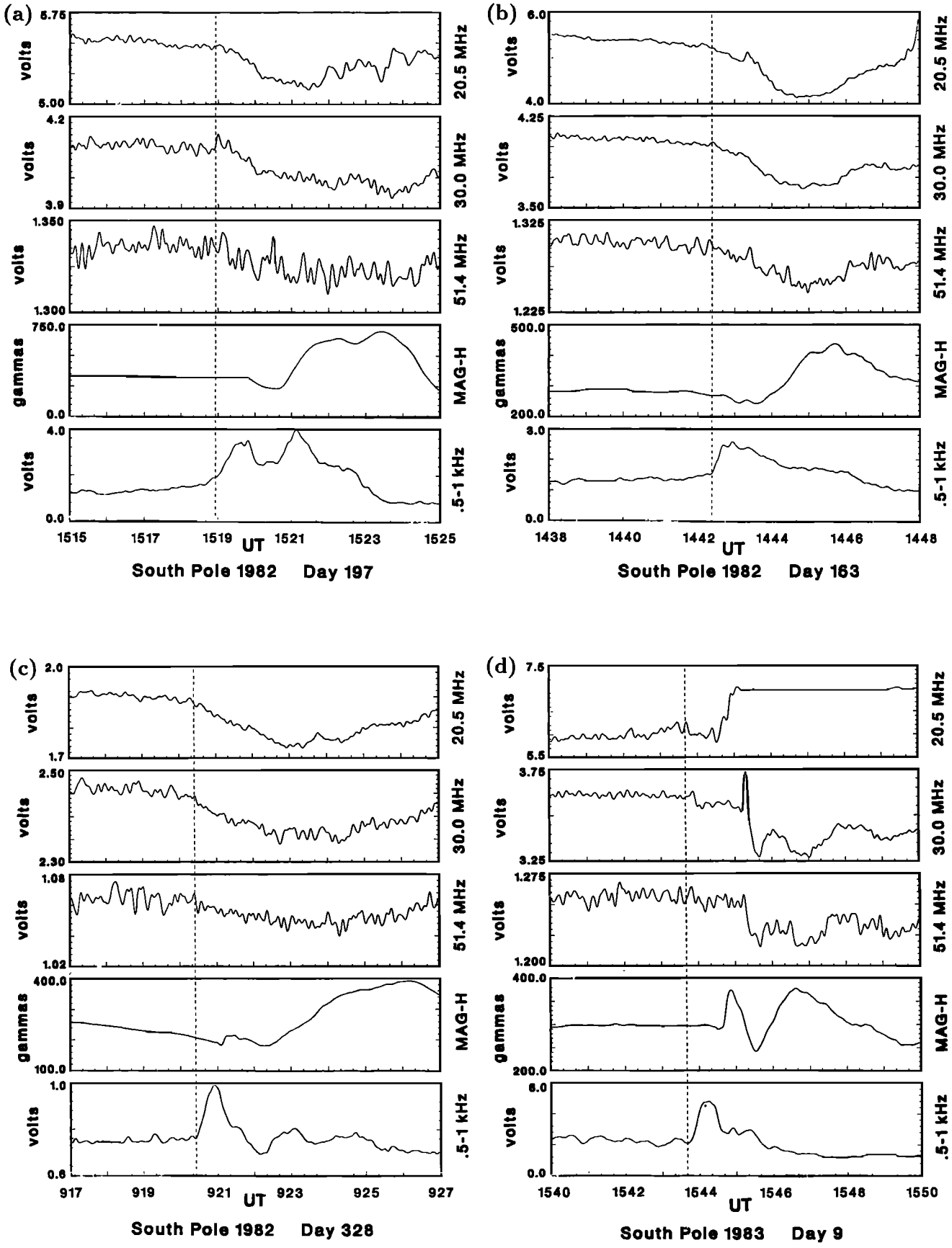

Fig. 12. Riometer data recorded at South Pole for four sc. Each panel shows the output of the 20.5-, 30.0-, and 51.4-MHz riometer channels as well as the magnetometer H component and the ELF amplitude in the 0.5- to 1-kHz channel. The dashed line indicates the wave growth onset.

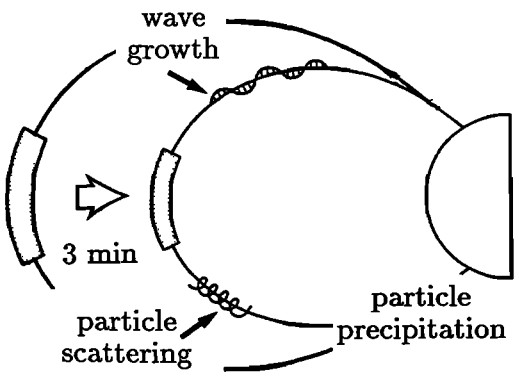

Fig. 13. Schematic diagram showing the displacement of a magnetic field line, the motion of the interaction region, and the corresponding consequences for the wave and particle populations.

azimuthal propagation of the sc disturbance) [*Kuwashima and Fukunishi*, 1985], while the ground magnetic onset occurs nearly simultaneously at all local times at high latitudes as a result of subionospheric transmission of the earliest arriving signal [*Kikuchi et al.*, 1978; *Kikuchi*, 1986].

The results presented here showed no apparent local time dependence for the onse t time of wave growth at South Pole when referenced to the arrival of the magnetic perturbation at the ground (Figure 11*a*) but a strong local time dependence when referenced to the magnetic perturbation at GOES (Figure 11*b*). The mean delay of 30 s between the onset of wave growth and the arrival of the ground magnetic perturbation is similar to the value of ~30 s measured by *Kuwashima and Fukunishi* [1985] for the propagation delay of the magnetic disturbance between GOES near local noon and ground observatories. The results are consistent with the source of the earliest ELF-VLF wave growth being near local noon.

Differences in the propagation path between events provide a possible explanation for the point scatter in Figure 11*a* (σ =18 s). Variations in the whistler mode delay (which is of the order of a few seconds) can probably be neglected, but significant variations in the propagation delay for Alfvén waves could be caused by differences in either the length of the propagation path or the integrated mass density along the path. A factor of 4 difference in integrated mass density between events would provide a sufficient variation in the propagation delay to account for the observed scatter. Differences in the location of the source region provide an alternate explanation. Using a mean Alfvén speed of 1000 km/s for the outer magnetosphere [*Wilken et al.*, 1982], a deviation of 18 s corresponds to variations of ± 3 R_E in radial position or ± 2 hours local time for the location of the earliest source region. It is probable that both effects play some role in determining the point scatter.

Particle precipitation measurements. Measurements of particle precipitation associated with sc provide a potentially powerful tool for determining the wave source regions. The 30° half-power beam width of the riometers corresponds to a field of view with a radius of about 60 km for absorption occurring at an altitude of 105 km. Since particles follow field-aligned paths from the interaction region to the ionosphere, riometer absorption associated with wave growth should provide a good indicator of the source region if the observed particles and waves can be associated with the same interaction region.

Previous work [*Ortner et al.*, 1962; *Hartz* 1963] has shown that riometer absorption is associated with sc at all local times and is generally limited to the geomagnetic latitude zone between 57° and 75°. Wave-induced particle precipitation is often assumed to be the cause of the absorption [*Leinbach et al.*, 1970; *Perona*, 1972], implying that changes in wave activity are triggered by the sc throughout a large portion of the inner magnetosphere. However, the problem has never been carefully studied, and other mechanisms (such as particle injection) may be responsible for some of the observed absorption effects.

The effect of other mechanisms can be minimized by analyzing absorption effects that occur during the first several tens of seconds of the sc. Of the 16 events discussed in section 3.6, five had well-defined absorption onsets (e.g., Figures 12*a-c*). In all five cases the absorption onset occurred simultaneously with the onset of ELF-VLF wave growth within an uncertainty of ± 10 s. Since the adiabatic changes in particle trajectories can only increase the pitch angle, adiabatic effects alone cannot increase the particle flux within the loss cone and thus cannot account for the absorption. With the assumed absence of other scattering mechanisms during the initial perturbation, the increased absorption is inferred to result from precipitation caused by interactions with the observed wave emissions.

The observation of wave-induced particle precipitation at South Pole implies that South Pole ($\Lambda = 73.8°$) was associated with closed field lines during these events (see *Brown* [1977] for a good discussion of the use of riometer observations during sc to detect the boundary of closed field lines). The local time at South Pole was within 2 hours of noon in four of the five cases. Since the closed field boundary in the noon region is nearly coincident with the magnetopause, the observation of wave-induced particle precipitation at South Pole suggests that an enhancement of wave-particle interactions occurs in a region extending to the vicinity of the dayside magnetopause.

In the four well-defined cases in which South Pole was near local noon, the approximate simultaneity of wave growth and absorption would be expected. The simultaneity in the fifth case (Figure 12*c*), for which the local time at South Pole was about 0550, cannot be easily explained. The wave growth and absorption onsets were observed at South Pole at 0920:25 UT, and the ground magnetic perturbation arrived at 0921:00 UT. The 35-s delay between the wave growth onset and the arrival of the magnetic perturbation is consistent with previous results, suggesting that the waves propagated subionospherically from a source region near noon. Precipitation effects due to these waves could not have been observed at South Pole (near dawn local time), however. Wave-induced precipitation should have been observed at South Pole with a delay of the order of 60 s (the propagation time for the magnetic disturbance between noon and dawn) after the disturbance began in the noon region. The magnetic perturbation arrived at GOES (0220 LT) at 0921:50, indicating that the perturbation could not have reached the dawn meridian prior to about 0921:10 (a time which would be consistent with the disturbance at local noon occurring at about 0920:25, the same time as the wave growth onset). The absorption observation for this event cannot be explained by wave-induced precipita-

tion triggered locally by the sc. An alternate explanation is that waves generated in the noon region propagated in a nonducted mode to the dawn region, in advance of the magnetic disturbance, where they interacted with and precipitated particles. Such a scheme seems rather unlikely, but raytracing has shown that nonducted waves generated in the noon region can propagate as far away as the dawn meridian [I. Kimura, private communication, 1987]. The "hybrid mode" [*Rastani et al.*, 1985], in which waves are ducted along some portions of a path and nonducted along others, could also be important in such azimuthal propagation. Although no other similar events were noted, the results suggest the possibility that precipitation could be observed at a given local time significantly in advance of when the sc disturbance reaches overhead field lines.

4.2. *Distribution of Source Regions*

Duct distribution. Knowledge regarding the occurrence of ducted propagation at high-latitude stations is limited. *Carpenter* [1981] studied whistlers from Byrd station and concluded that ducted propagation of whistlers at equatorial distances of 6-8 R_E is probably observed on 30-50% of all days and that chorus and hiss propagate at equatorial distances 0.5-1.0 R_E beyond the observed limit of whistler propagation on the dayside. The common occurrence of polar chorus at high latitudes is also strong, though indirect, evidence that ducts ordinarily exist at equatorial distances greater than 6 R_E. These considerations support the results discussed in section 4.1 suggesting that wave growth during sc could originate in ducts near the dayside magnetopause.

The number of ducts contributing to the wave signal observed at ground stations during sc is difficult to determine. The large viewing area of ground-based receivers allows for superposition of wave activity from different ionospheric exit points and thus makes distinction of multiple source regions difficult. Comparison of data from stations separated by distances of the order of the viewing radius (~1500 km in the magnetic north-south direction; e.g., South Pole and Siple) allows for some resolution of this problem. As shown in Figure 3, spectra at Siple and South Pole appeared similar in many cases (including correlated discrete emissions as in Figures 3*b* and 3*d*), but showed clear differences in other cases. In at least one case, similar polar chorus bands with a UCF near 500 Hz were observed at both stations while a hiss band with a UCF above 5 kHz was observed at Siple but not South Pole. In those cases with similar spectra particularly when similar emissions were identified, it is probable that both stations were viewing the same wave source regions, but the number of such regions cannot be determined. In those cases with different spectra it appears that the stations were viewing at least two different source regions, although some overlap is possible.

Sensitivity to source distribution. While the observations do not resolve the question of the number of ELF-VLF source regions, there is a simple argument suggesting that the measured growth values are not very sensitive to the number of contributing source regions or ducts. Three primary factors affect the contribution of a particular source region to the observed ELF-VLF wave growth: the relative wave amplitude, the relative growth rate, and the relative onset time of the growth for a particular source region. Source regions with small relative wave amplitudes compared to other source regions will not be important. Source regions with small relative growth rates will also be insignificant since they will contribute less and less to the total signal amplitude with time. Differences in relative onset time (due, for instance, to different radial positions of the source regions) would result in larger comparative wave amplitudes for those signals with the earliest growth onset, and these signals would provide the greatest contribution.

Signals with the highest initial amplitudes and growth rates and the earliest growth onsets thus dominate the observed wave growth process. A given source distribution, however, may have no one source which dominates all three categories. To investigate this further, a simple computer simulation of the contribution of a number of ducts with different initial wave amplitudes, growth rates, and radial positions was conducted. The results showed that the measured values of growth rate and total growth are only weakly dependent on the number and distribution of source regions. The variation from a wide range of simulated cases was comparable to the observed variation in the measured values.

4.3. *Propagation Effects*

Since we use relative rather than absolute measurements of wave properties, only those propagation effects which change during the sc are of interest. The effects which must be considered include propagation within the duct, transmission through the ionosphere, and propagation from the ionospheric exit point to the receiver.

The frequency at which waves remain trapped within an enhancement duct is theoretically limited by refractive index effects to $f < f_H/2$ [*Helliwell*, 1965]. During an sc the frequency range for ducted propagation thus increases in proportion to the gyrofrequency. The range of possible wave normal angles, which is described by the ratio of the electron densities inside and outside the duct [*Helliwell*, 1965], changes appreciably only for $f \simeq f_H/2$. Scattering losses from the duct are generally considered to be negligible except for frequencies near $f_H/2$ [*Scarabucci and Smith*, 1971; *Karpman and Kaufman*, 1984].

Observations of enhanced riometer absorption during sc suggest that ionospheric absorption losses for ELF-VLF waves should also increase. Additional absorption losses would reduce values for growth rate and total growth measured at ground stations. The spectral distribution would not be significantly modified, however, since absorption losses at the wave frequencies of interest are proportional to $\sqrt{f}$ [*Helliwell*, 1965] and would result in less than 3 dB of differential absorption over the frequency range 0.5-4.0 kHz. Quantitative absorption values, which depend on both the flux and energy spectrum of the precipitated particles, are very difficult to determine. For the growth period measurements, made within the first several tens of seconds of the event, the absorption was in general significantly less than the value measured at the absorption maximum. It is probably reasonable to assume that measurements made during the growth period are not significantly affected by changes in ionospheric absorption losses or changes in propagation losses between the ionospheric exit point and the receiver.

5. SUMMARY AND CONCLUSIONS

The occurrence statistics suggest that the magnetic field and plasma perturbations associated with sc are sufficient

to cause measurable modification of the gyroresonance process during at least 80% of sc. The amplitude response is characterized by a transient enhancement lasting 1-8 min after which the amplitude is usually reduced to below the pre-sc amplitude but may be significantly higher than the pre-sc level. Ionospheric absorption losses corresponding to the observed riometer absorption provide a possible explanation for amplitude reductions, although the continued amplitude reduction in a number of cases following the riometer recovery as well as the clear change in the spectra suggest that ionospheric absorption is not the primary cause. Damped oscillations with period 60-90 s are commonly observed during the transient enhancement. The oscillations may be associated with resonant field line oscillations, although the evidence is not clear. An alternate explanation is that they represent an overshoot and subsequent oscillation of the wave amplitude about the new equilibrium value with a period determined by time scales associated with the wave-particle interaction mechanism.

Wave activity associated with sc usually involves amplitude and spectral modification of preexisting bands of polar chorus or mid-latitude hiss in the frequency range 0-5 kHz. During the growth period the upper cutoff frequency of the wave activity increases by a factor of 1.3-2.8. In some cases, the lower cutoff frequency increases as well. Growth is observed first at lower frequencies and with increasing delay (of the order of 10- to 35-s) at higher frequencies. The onset of ionospheric absorption measured by riometers was found to occur within ±5 s of the earliest wave growth observations in the most well-defined cases, suggesting that the absorption results from wave-induced scattering of electrons. The 10- to 35-s time delay is significantly shorter than the typical sc rise time (2-6 min), so the increase is probably not simply due to the change in $f_{H_{eq}}$ for a single duct. A possible explanation is that wave growth is triggered in ducts with successively higher values of $f_{H_{eq}}$ as the disturbance propagates radially earthward. An alternate explanation is that the upper cutoff frequency is not controlled by $f_{H_{eq}}$ but is a function of other medium parameters. The narrow-band growth rate (0.3-2.7 dB/s) and total growth (12-29 dB) are independent of frequency over a bandwidth of 0.4-1.2 kHz and a dynamic range of as much as 20 dB. This growth rate is at least 2 orders of magnitude less than known growth rates for coherent waves [*Burtis and Helliwell*, 1975; *Stiles and Helliwell*, 1977]. Triggering of discrete emissions is observed in some cases. Onset time measurements indicate that waves observed during the growth phase correspond to contributions from wave sources in the noon region, probably outside the plasmapause and possibly in some cases from near the magnetopause. A measurable enhancement of ionospheric absorption due to pitch angle scattering of electrons commonly accompanies the growth process.

Acknowledgments. We would like to thank J. Katsufrakis for his helpful comments, J. Yarbrough for assistance in data preparation, and the many field observers who collected the data. The work at Stanford was sponsored by the Division of Polar Programs of the National Science Foundation under grant DPP 8613783 for work at Siple Station and earlier grants for work at South Pole and Palmer Stations. The University of Maryland riometer data acquisition was supported under grants DPP 8304844 and DPP 8610061. Logistic support for the Bell Laboratories magnetometers was provided by the Division of Polar Programs of the National Science Foundation. The GOES magnetometer data were obtained with the assistance of World Data Center-A in Boulder, Colorado.

The Editor thanks L. J. Cahill, Jr., and H. J. Strangeways for their assistance in evaluating this paper.

REFERENCES

Barfield, J. N., and P. J. Coleman, Storm-related wave phenomena observed at the synchronous, equatorial orbit, *J. Geophys. Res., 75*, 1943, 1970.

Baumjohann, W., O. H. Bauer, G. Haerendel, and H. Junginger, Magnetospheric plasma drifts during a sudden impulse, *J. Geophys. Res., 88*, 9287, 1983.

Baumjohann, W., H. Junginger, G. Haerendel, and O. H. Bauer, Resonant Alfvén waves excited by a sudden impulse, *J. Geophys. Res., 89*, 2765, 1984.

Brown, R. R., Sudden commencement absorption events at the edge of the polar cap, *J. Geophys. Res., 82*, 2433, 1977.

Brown, R. R., T. R. Hartz, B. Landmark, H. Leinbach, and J. Ortner, Large-scale electron bombardment of the atmosphere at the sudden commencement of a geomagnetic storm, *J. Geophys. Res., 66*, 1035, 1961.

Burtis, W. J., and R. A. Helliwell, Magnetospheric chorus: Amplitude and growth rate, *J. Geophys. Res., 80*, 3265, 1975.

Carpenter, D. L., A study of the outer limits of ducted whistler propagation in the magnetosphere, *J. Geophys. Res., 86*, 839, 1981.

Cornilleau-Wehrlin, N., J. Solomon, A. Korth, and G. Kremser, Experimental study of the relationship between energetic electrons and ELF waves observed on board GEOS: A support to quasi-linear theory, *J. Geophys. Res., 90*, 4141, 1985.

Fukunishi, H., Latitude dependence of power spectra of magnetic pulsations near $L = 4$ excited by ssc's and si's, *J. Geophys. Res., 84*, 7191, 1979.

Gail, W. B., and U. S. Inan, Characteristics of wave-particle interactions during sudden commencements, 2, Spacecraft observations, *J. Geophys. Res.*, this issue.

Hartz, T. R., Multi-station riometer observations, in *Radio Astronomical and Satellite Studies of the Atmosphere*, edited by J. Aarons, North-Holland, Amsterdam, 1963.

Hayashi, K., S. Kokubun, and T. Oguti, Polar chorus emission and worldwide geomagnetic variation, *Rep. Ionos. Space Res. Jpn., 22*, 149, 1968.

Helliwell, R. A., *Whistlers and Related Ionospheric Phenomena*, Stanford University Press, Stanford, Calif., 1965.

Hirasawa, T., Effects of magnetospheric compression and expansion on spectral structure of ULF emissions, *Mem. Natl. Inst. Polar Res. Spec. Issue Jpn., 18*, 127, 1981.

Karpman, V. I., and R. N. Kaufman, Whistler wave propagation in magnetospheric ducts (in the equatorial region), *Planet. Space Sci., 32*, 1505, 1984.

Kennel, C. F., and H. E. Petschek, Limit on stably trapped particle fluxes, *J. Geophys. Res., 71*, 1, 1966.

Kikuchi, T., Evidence of transmission of polar electric fields to the low latitude at times of geomagnetic sudden commencements, *J. Geophys. Res., 91*, 3101, 1986.

Kikuchi, T., T. Araki, H. Maeda, and K. Maezawa, Transmission of polar electric fields to the equator, *Nature, 273*, 650, 1978.

Kokubun, S., Characteristics of storm sudden commencement at geostationary orbit, *J. Geophys. Res., 88*, 10,025, 1983.

Kokubun, S., and T. Oguti, Hydromagnetic emissions associated with Storm sudden Commencements, *Rep. Ionos. Space Res. Jpn., 22*, 45, 1968.

Korth, A., G. Kremser, N. Cornilleau-Wehrlin, and J. Solomon, Observations of energetic electrons and VLF waves at geostationary orbit during storm sudden commencements (ssc), paper presented at *Chapman Conference on Solar Wind — Magnetosphere Coupling*, AGU, Pasadena, Calif., 1985.

Kuwashima, M., and H. Fukunishi, Local time asymmetries of the ssc-associated hydromagnetic variations at the geosynchronous altitude, *Planet. Space Sci., 33*, 711, 1985.

Leinbach, H., R. J. Schmidt, and R. R. Brown, Conjugate observations of an electron precipitation event associated with the sudden commencement of a magnetic storm, *J. Geophys. Res., 75*, 7099, 1970.

Morozumi, H. M., Enhancement of VLF chorus and ULF at the time of sc, *Rep. Ionos. Space Res. Jpn., 19*, 371, 1965.

Oguti, T., and S. Kokubun, Hydromagnetic emissions in high lat-

itudes associated with storm sudden commencements, II, *Rep. Ionos. Space Res. Jpn., 23*, 162, 1969.

Olson, J. V., and L. C. Lee, Pc1 wave generation by sudden impulses, *Planet. Space Sci., 31*, 295, 1983.

Ortner, J., B. Hultqvist, R. R. Brown, T. R. Hartz, O. Holt, B. Landmark, J. L.

Hook, and H. Leinbach, Cosmic noise absorption accompanying geomagnetic storm sudden commencements, *J. Geophys. Res., 67*, 4169, 1962.

Perona, G. E., Theory on the precipitation of magnetospheric electrons at the time of a sudden commencement, *J. Geophys. Res., 77*, 101, 1972.

Rastani, K., U. S. Inan, and R. A. Helliwell, DE 1 observations of Siple transmitter signals and associated sidebands, *J. Geophys. Res., 90*, 4128, 1985.

Sakurai, T., Y. Tonegawa, K. Tomomura, and Y. Kato, A multisatellite study of magnetic pulsations associated with a storm sudden commencement (ssc) as observed at synchronous orbit, *Mem. Natl. Inst. Polar Res. Spec. Issue Jpn., 31*, 1, 1984.

Scarabucci, R. R., and R. L. Smith, Study of magnetospheric field oriented irregularities — the mode theory of bell-shaped ducts, *Radio Sci., 6*, 65, 1971.

Schulz, M., and L. J. Lanzerotti, *Particle Diffusion in the Radiation Belts*, Springer-Verlag, New York, 1974.

Stiles, G. S., and R. A. Helliwell, Stimulated growth of coherent VLF waves in the magnetosphere, *J. Geophys. Res., 82*, 532, 1977.

Tepley, L. R., and R. C. Wentworth, Hydromagnetic emissions, X-ray bursts, and electron bunches, 1, Experimental results, *J. Geophys. Res., 67*, 3317, 1962.

Tsuruda, K., S. Machida, T. Terasawa, A. Nishida, and K. Maezawa, High spatial attenuation of the Siple transmitter signal and natural VLF chorus observed at ground-based chain stations near Roberval, Quebec, *J. Geophys. Res., 87*, 742, 1982.

Tsurutani, B. T., S. R. Church, and R. M. Thorne, A search for geographic control of the occurrence of magnetospheric ELF emissions, *J. Geophys. Res., 84*, 4116, 1979.

Ullaland, S. L., K. Wilhelm, J. Kangas, and W. Riedler, Electron precipitation associated with a sudden commencement of a geomagnetic storm, *J. Atmos. Terr. Phys., 32*, 1545, 1970.

Walker, A. D. M., Excitation of the earth-ionosphere waveguide by downgoing whistlers, II, Propagation in the magnetic meridian, *Proc. R. Soc. London, Ser. A.*, 340, 1974.

Wedeken, U., H. Voelker, K. Knott, and M. Lester, ssc-excited pulsations recorded near noon on GEOS 2 and on the ground (CDAW 6), *J. Geophys. Res., 91*, 3089, 1986.

Wilken, B., C. K. Goertz, D. N. Baker, P. R. Higbie, and T. A. Fritz, The ssc on July 29, 1977 and its propagation within the magnetosphere, *J. Geophys. Res., 87*, 5901, 1982.

Wilson, C. R., and M. Sugiura, Hydromagnetic interpretation of sudden commencements of magnetic storms, *J. Geophys. Res., 66*, 4097, 1961.

D. L. Carpenter, R. A. Helliwell, and U. S. Inan, Space, Telecommunications, and Radioscience Laboratory, Stanford University, Stanford, CA 94305.

W. B. Gail, The Aerospace Corporation, P.O. Box 92957, Los Angeles, CA 90009.

S. Krishnaswamy, National Space Science Data Center, Greenbelt, MD 20771.

L. J. Lanzerotti, AT&T Bell Laboratories, Murray Hill, NJ 07974.

T. J. Rosenberg, Institute for Physical Science and Technology, University of Maryland, College Park, MD 20742.

(Received October 17, 1988;
revised January 30, 1989;
accepted February 2, 1989.)